# Picosecond Time-Resolved Fluorescence Studies on Excitation Energy Transfer in a Histidine 117 Mutant of the D2 Protein of Photosystem II in *Synechocystis* 6803†

Sergei Vasil'ev* and Doug Bruce

*Department of Biological Sciences, Brock University, St. Catharines, Ontario L2S 3A1, Canada*

*Received March 1, 2000; Revised Manuscript Received September 7, 2000*

ABSTRACT: The role of the peripheral reaction center chlorophyll *a* molecule associated with His117 of the D2 polypeptide in photosystem II was investigated in *Synechocystis* sp. PCC 6803 using a combination of steady state, pump−probe, and picosecond time-resolved fluorescence spectroscopy. Data were obtained from intact cells and isolated thylakoid membranes of a control mutant and a D2-H117T mutant, both of which lacked photosystem I. Excitation energy transfer and trapping were investigated by analyzing the data with a kinetic model that used an exact numerical solution of the Pauli master equation, taking into account available photosystem II spectral and structural information. The results of our kinetic analysis revealed the observed difference in excited-state dynamics between the H117T mutant and the control to be consistent with a retardation of the rate of excitation energy transfer from the peripheral chlorophyll of D2 (Chl at His117) to the electron-transfer pigments and an increase of the rate constant for charge recombination in the H117T mutant. The kinetic model was able to account for the experimentally observed changes in absorption cross section and fluorescence decay kinetics between the control and mutant by invoking changes in only these two rate constants. The results rule out quenching of excitation by a chlorophyll cation radical as a mechanism responsible for the lower efficiency of excitation energy utilization in the H117T mutant. Our work also demonstrates the importance of the chlorophyll associated with His117 of the D2 protein for excitation energy transfer to the PSII electron-transfer pigments and for the effective stabilization of the primary radical pair.

Photosystem II (PSII)[1] is a membrane-bound multisubunit pigment−protein complex capable of producing the very high redox potential required for photochemical water oxidation. Native PSII is comprised of more than 25 different protein subunits (*1*). The light-induced charge separation which initiates the sequence of electron transport reactions across the thylakoid membrane occurs in the reaction center of PSII, which consists of the D1, D2 polypeptides and cytochrome *b*-559 (*2*). The chlorophyll-binding proteins CP47 and CP43 are closely associated with the D1−D2−cyt $b_{559}$ complex and are involved in both light harvesting and transfer of excitation energy from the outer light-harvesting antenna complexes (LHCII) to the reaction center (*3*). The D1 and D2 proteins are structurally and functionally homologous to the L and M subunits of the reaction center of purple nonsulfur bacteria (BRC) and have been predicted to hold the active pigments in a similar configuration (*4*−*6*). However, the chlorophyll composition of the D1−D2−cyt $b_{559}$ complex and the BRC is different: the reaction center of PSII binds six chlorophylls (*7*−*10*), while the BRC contains only four bacteriochlorophylls. It has been speculated by a number of groups that the histidines (common ligands to chlorophyll) at positions D1−118 and D2−117 are the binding sites of these two extra "accessory" chlorophylls in the reaction centers of PSII *(6, 9, 11*−*13)*. Later, site-directed mutations confirmed this assignment and provided evidence that H118 of D1 and H117 of D2 are the axial ligands to accessory chlorophylls, $Chl_Z$ and $Chl_D$ correspondingly (*14*). Substitution of His with noncoordinating or poorly coordinating residues at either position decreased photosynthetic competence and impaired assembly of PSII complexes (*14*−*16*). The mutants that retained photoautotrophic growth had residues at the D2−117 position that could serve as chlorophyll ligands. One of these mutants, the mutant with threonine at the D2−117 position exhibited pronounced phenotypic changes compared with the wild type: (i) a large decrease in 77 K fluorescence emission at 695 nm; (ii) a decrease of variable fluorescence at room temperature; (iii) a decreased PSII quantum yield (*16*). Thus, mutation of a single amino acid in the reaction core of PSII was found to induce dramatic changes in excited-state dynamics and electron transport in PSII. On the basis of these findings and the location of His117 at the periphery of the D1−D2−cyt $b_{559}$ complex, Lince and Vermaas (*16*) suggested that chlorophyll associated with His117 is important for the efficient excitation transfer between the proximal antenna (CP43 and CP47) and the reaction center. They also pointed out that a decreased efficiency of energy transfer to PSII

† Supported by operating and equipment grants from the Natural Sciences and Engineering Research Council of Canada (NSERC) to D.B.

* Address correspondence to this author. Tel: (905) 688-5550 ext 4163. Fax: (905) 688-1855. E-mail: svassili@spartan.ac.brocku.ca.

[1] Abbreviations: PS, photosystem; LHCII, light-harvesting chlorophyll-binding antenna complex associated with photosystem II; BRC, reaction center of purple bacteria; fwhm, full width at half-maximum; APC, allophycocyanin; DAS, decay-associated spectrum; PAM, pulse amplitude modulated fluorometry; $F_0$, minimal fluorescence yield; $F_m$, maximal fluorescence yield; RRP, reversible radical pair.

10.1021/bi000476v CCC: $19.00 
Published on Web 10/26/2000

reaction centers in H117T mutants could be ascribed to quenching of excitations by a chlorophyll cation, possibly associated with the His117 residue of the D2 protein, which accumulates in mutants with a higher efficiency than in the control.

In this paper we present a detailed picosecond time-resolved fluorescence study of the D2 H117T mutant of *Synechocystis* sp. PCC 6803 aimed at understanding the molecular mechanism behind the previously observed changes in excited-state dynamics in these mutants. The decay-associated emission spectra obtained from the intact mutant cells and isolated thylakoid membranes were analyzed with a kinetic model that utilized an exact numerical solution of the Pauli master equation and took into account a realistic structural model of PSII based on the recent electron crystallographic studies of Barber (*17*, *18*). The results of our kinetic analysis show that the observed difference in excited-state dynamics between the H117T mutant and the control can be explained by a change of the orientation of the chlorophyll associated with the His117 D2, resulting in the retardation of the rate of excitation energy transfer from this chlorophyll to the reaction center core pigments and an increase of the rate constant for charge recombination in the PSII reaction center of the H117T mutant.

## MATERIALS AND METHODS

*Samples.* The PSI-less strain and H117T mutant, derived from this strain, were grown at 30 °C in BG-11 medium in the presence of 15 mM glucose at a light intensity of 5 $\mu$E $m^{-2}$ $s^{-1}$ (*16*). The thylakoid membranes were prepared from cells according to the method of Diner et al. (*19*). Directly after isolation the samples were frozen in liquid nitrogen and stored at −80 °C.

*Absorption Cross Sections.* Pump−probe fluorometry was used for the determination of relative PSII absorption cross sections from flash saturation curves of fluorescence as previously outlined (*20*) with some modifications. Nonactinic probe pulses of light were supplied by a blue LED focused onto a 1 mm diameter flow cuvette with a circulating sample (0.7 mL $s^{-1}$ pumping rate). Actinic pump pulses (300 ps fwhm), generated by a nitrogen-pumped dye laser (Photon Technologies International, GL-3300) set at 440, 630, or 655 nm, were delivered 70 $\mu$s before the probe LED flashes. Fluorescence was measured at 90° to the direction of the incident pump-and-probe flashes using a photomultiplier protected with a 690 nm long pass filter. Each data point consisted of an average of 30 signals collected at a flash frequency of 2 Hz. Data were fit with the cumulative Poisson single-hit probability distribution (*21*).

*Time-Resolved Fluorescence Measurements.* Fluorescence decay kinetics were measured with the single photon timing apparatus previously described (*22*). Excitation was at 664 nm with a repetition rate of 10 MHz. The fwhm of the system response function was about 80 ps. Fluorescence decays were recorded for several emission wavelengths at a resolution of 12 ps/channel, resulting in a total time window of 12 ns. For $F_0$ measurements thylakoid samples were circulated through a 1 mm diameter flow cuvette with a flow rate of 4.2 mL $s^{-1}$. The $F_m$ state was achieved by addition of DCMU and illumination of the sample in a small preillumination chamber for about 400 ms just prior to measurement. In all experiments with thylakoids, the bulk of data collection was completed within 15 min of removing samples from ice to avoid sample destabilization. For the low-temperature measurements the samples were mixed with 1 M sucrose to a final concentration of about 1 $\mu$M Chl and were shock frozen by dipping in liquid nitrogen in a 1 mm capillary tube.

*Global Lifetime Analysis.* Our use of global lifetime analysis as well as its application for quantification of the PSI, PSII-α, and $\beta$ fluorescence decay components has been outlined previously (*22*, *23*). In the present study we used a similar approach to analyze the fluorescence decay kinetics of intact *Synechococcus* cells and isolated thylakoids. However, especially with the intact cyanobacteria, we encountered the nontrivial problem of extracting the PSII decay components from the fluorescence decay kinetics obtained in a very congested lifetime-wavelength domain with strong contributions from phycobilin pigments. To solve this problem, we extended the range of detection to 640−730 nm with 15 detection wavelengths to safely cover emission of all phycobilins and chlorophylls in the system and applied a simultaneous global analysis of the decay kinetics recorded at the $F_0$ and $F_m$ states. At the $F_0$ state the fast ($\tau \sim 200$ ps) decay component contains contributions from PSII decay, allophycocyanin (APC) decay, and APC−PSII energy transfer (*24*, *25*), while at the $F_m$ state a decay component with very similar lifetime is dominated by only the latter two processes (at $F_m$ the PSII reaction centers decay much more slowly). Thus measurements at $F_m$ were used to determine the contribution of the APC decay and APC−PSII energy transfer to the decay kinetics at $F_0$. An additional approach utilized decomposition of DAS measured at $F_0$ into phycobilin and chlorophyll spectral components. The shape of the PSII-related component was found from the DAS of the major decay component at $F_m$. The phycobilin emission spectrum was measured from supernatant obtained in the course of thylakoid isolation.

*Kinetic Modeling.* To facilitate the kinetic modeling of PSII, we first extracted the PSII-associated decay components from the fluorescence decays at all detection wavelengths and quenching conditions by doing a global analysis using a sum of exponential decays. The lifetimes and corresponding decay-associated spectra (DAS) for the PSII-associated components were then used as parameters to describe the fluorescence decay kinetics of PSII alone. This "isolated" PSII decay was then reproduced with the reversible radical pair model (RRP), which takes into account reversibility of primary charge separation and fast establishment of exciton equilibration in PSII (*26*). Finally, we introduced a detailed kinetic model of PSII containing all of the chlorophyll molecules located within the D1−D2−CP43−CP47 complex. The details of the procedure we used to describe the excited-state dynamics in this system of chlorophyll molecules have been described previously (*26*, *27*) and will be summarized here briefly.

The excited-state migration and trapping in an array of fluorescing molecules is governed by a system of linear differential equations. The Pauli master equation describing a system of $N$ pigments is given by

$$\frac{d\mathbf{p}}{dt} = \langle \mathbf{W} \rangle \mathbf{p}(t) \qquad (1)$$

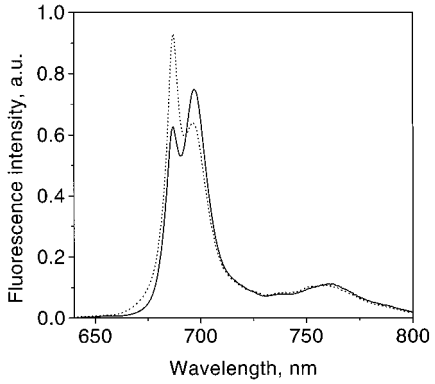


FIGURE 1: Low-temperature fluorescence emission spectra of the H117T mutant in PSI-less background (dashed line) and the PSI-less control (solid line) thylakoids.

where $p_i(t)$ is the probability that molecule $i$ is excited at time $t$, vector $\mathbf{p}(t)$ is defined as a set of $N$ probabilities $p_i(t)$, and $\langle \mathbf{W} \rangle$ is an $N \times N$ transfer matrix for the system which contains the energy and electron-transfer rates. This equation has the solution:

$$\mathbf{p}(t) = \mathbf{p}(0) \exp(-\langle \mathbf{W} \rangle t) \quad (2)$$

which can be expressed in terms of the matrix elements:

$$p_i(t) = c_1 x_{il} \exp(\lambda_1 t) + c_2 x_{i2} \exp(\lambda_2 t) + ... + c_N x_{iN} \exp(\lambda_N t) \quad (3)$$

where $\lambda_i$ are the eigenvalues of the rate matrix, $x_{ij}$ are the eigenvector elements corresponding to pigment $i$ and eigenvalue $j$, and $c_j$ are the constants determined such that $p_i(0)$ terms are equal to the initial distribution of excitation in the system. To fit the model kinetics to experimental time-resolved fluorescence data, $p_i(t)$ were obtained from the numerical solution of eq 1. The calculated fluorescence decay curves are given then as

$$F(\lambda_{em}, t) = \sum_i f_i(\lambda_{em}) P_i(t) \quad (4)$$

where $f_i$ is the emission spectrum of the $i$th pigment.

## RESULTS

*Variable Fluorescence.* In good agreement with the previous study by Lince and Vermaas (*16*), H117T cells showed a decrease of 77 K fluorescence yield at 695 nm relative to 685 nm (Figure 1). Variable Chl *a* fluorescence was measured using pulse amplitude modulated (PAM) fluorometry, and again the same decrease in $F_m/F_0$ as reported earlier (from 2.2 to 1.3) was found (data not shown). In an attempt to clarify whether the variable fluorescence from H117T mutants decreased because $F_0$ was elevated or because $F_m$ was quenched, we performed time-resolved fluorescence decay measurements. Typical fluorescence decay kinetics of control and H117T cells for the $F_0$ and $F_m$ states measured at 685 nm are shown in Figure 2. The fluorescence decays measured at $F_m$ were almost identical, indicating that there was no additional quenching of excitation energy in the H117T mutant. This result does not support the previously suggested idea that a Chl cation generated in PSII at $F_m$ is responsible for the decreased $F_m/F_0$ ratio in the H117T mutant. Furthermore, the fluorescence decay at

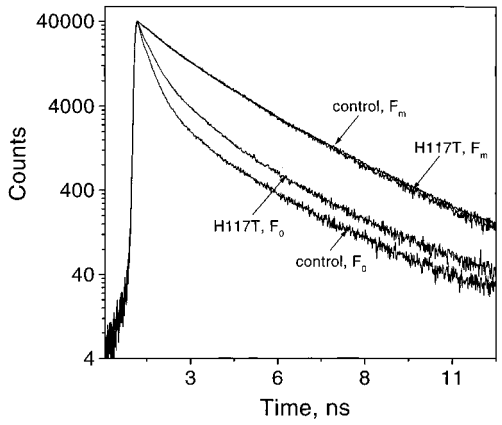


FIGURE 2: Fluorescence decay kinetics of the PSI-less control and H117T mutant in PSI-less background cells for the $F_0$ and $F_m$ states measured at 685 nm at room temperature. See text for details.

$F_0$ was considerably slower in the H117T mutant cells than in the control cells, indicating that the decreased $F_m/F_0$ ratio in H117T cells arises from an increase in the amplitude of $F_0$.

*Fluorescence Decay Kinetics.* To clarify the origin of the slower decay at $F_0$ in H117T, we performed a global lifetime analysis of fluorescence decay kinetics of both PSI and PSI/PSII-less controls and the H117T mutant. The PSI/PSII-less cells have previously been characterized as containing approximately 20% of the Chl found in the PSI-less cells (*16*). Fluorescence decay curves were recorded at six detection wavelengths between 659 and 695 nm for isolated thylakoids at $F_0$ at room temperature. The fluorescence decay data were analyzed globally by fitting to a sum of exponential decays to obtain lifetimes and corresponding DAS.

Two lifetimes ($\tau_1 = 1.3$ ns, $A_1 = 62\%$; $\tau_2 = 2.1$ ns, $A_2 = 38\%$) were required to describe the decay kinetics of the PSI/PSII-less control ($\chi^2 = 1.08$). Both decay components had similar DAS with maxima around 685 nm, suggesting a single pool of chlorophyll-containing complexes with a mean lifetime $\tau_{mean} = 1.8$ ns (data not shown).

Five lifetimes were required to describe the decay curves of both the PSI-less control and the H117T mutant (Figure 3, $\chi^2 = 1.1$). The shortest lifetime component was assigned to exciton equilibration within the antenna complexes. The second and the third decay components ($\tau_2 = 90-100$ ps and $\tau_3 = 490-540$ ps) had similar DAS peaking at 685 nm and were assigned to PSII with open reaction centers. The lifetimes and amplitudes of the two PSII-associated decay components were different in the H117T mutant and the PSI-less control, indicating differences in excitation transfer and/or primary photochemistry in PSII. The fourth component had a lifetime ($\tau_4$) of ~1.8 ns and peaked at about 675 and 685 nm. This component was very similar to the decay we observed in the PSI/PSII-less strain. We therefore assign the fourth decay component to this "additional" chlorophyll. As the lifetimes of this component were very close to the mean lifetime of the fluorescence decay of the PSI/PSII-less control, we assume this chlorophyll complex does not transfer excitation to PSII. The fifth component ($\tau_5 = 4-6$ ns) had a very small relative amplitude and was assigned to emission from excitonically disconnected pigments.

Lifetimes and amplitudes of the PSII decay components separated from other components and assigned to open

Table 1: Parameters of PSII Fluorescence Decay Components and Rate Constants for Primary Processes Obtained from the Global Lifetime Analysis and Kinetic Modeling of the Experimental Data[a]

| sample | $\tau_1$, ns ($A_1$, %) | $\tau_2$, ns ($A_2$, %) | $\tau_3$, ns ($A_3$, %) | $k_A$, $ns^{-1}$ | $k_{PC}$, $ns^{-1}$ | $k_{PC}^{trap}$, $ns^{-1}$ | $k_{PC}^{-}$, $ns^{-1}$ | $k_{ST}$, $ns^{-1}$ | $k_{ChlHis117\rightarrow RC}$, $ns^{-1}$ |
|---|---|---|---|---|---|---|---|---|---|
| | | | (A) Simple RRP Model—Thylakoids | | | | | | |
| control | n/a | 0.09 (79) | 0.49 (21) | 0.3 | n/a | 8.9 | 1.5 | 2.4 | n/a |
| H117T | n/a | 0.1 (68) | 0.54 (32) | 0.3 | n/a | 7.1 | 2.0 | 2.4 | n/a |
| | | | (B) Detailed Kinetic Model—Thylakoids | | | | | | |
| control | 0.01 (43) | 0.09 (45) | 0.49 (12) | 0.3 | 940 | n/a | 5.9 | 2.3 | 118 |
| H117T | 0.01 (40) | 0.1 (41) | 0.54 (19) | 0.3 | 940 | n/a | 7.3 | 2.2 | 42 |
| | | | (C) PSII Decay Components—Intact Cells | | | | | | |
| control | 0.01 (44) | 0.18 (44) | 0.5 (12) | | | | | | |
| H117T | 0.01 (42) | 0.19 (36) | 0.62 (22) | | | | | | |

[a] $\tau_2$ and $\tau_3$ are the fast and slow PSII-associated decay components whose complete decay associated spectra (DAS) are shown in Figure 3 (see text for details). The data presented are the means of three independent experiments. The uncertainty in lifetimes and amplitudes is 10%.

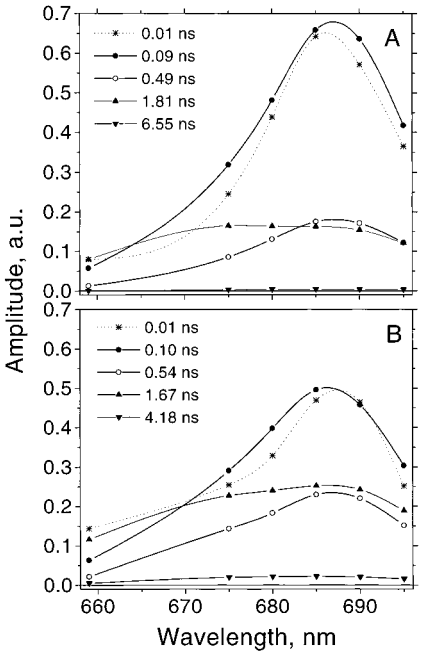


FIGURE 3: Decay-associated spectra obtained from a global multiexponential decay analysis of fluorescence kinetics of the control (A) and mutant (B) thylakoids recorded at room temperature in the range of 659−695 nm.

reaction centers are compiled in Table 1. PSII decay parameters of the control thylakoids were in agreement with previous studies of PSII particles (*28*, *29*). The major difference between control and H117T thylakoids was an increase in the amplitude and lifetime of the slow ($\tau_3$) PSII component.

Fluorescence decay kinetics of the intact cells were more complex than those from isolated thylakoid membranes, as they also contained large multiexponential contributions from phycobilisomes. Nevertheless, determination of PSII decay kinetics in intact cells was important as we wanted to ensure that (i) retardation of the rate of PSII decay in the H117T mutants was not due to an altered interaction between PSII and phycobilisomes and (ii) electron-transfer reactions in the reaction centers of PSII were not modified by the thylakoid isolation procedure. We were able to separate PSII decay kinetics by extending the range of detection from 640 to 730 nm and applying a simultaneous global analysis of the decay kinetics recorded at the $F_0$ and $F_m$ states (procedure described in Materials and Methods). The lifetimes and amplitudes of the PSII decay components obtained from analysis of the data for intact cells and isolated thylakoids (see Table 1) were very similar. This result implies that the effect of the H117T mutation on fluorescence decay kinetics did not arise from a modified interaction between PSII and phycobilisomes and that reaction centers in isolated thylakoids were not altered by the isolation procedure.

The lifetimes and corresponding DAS resulting from the global analysis were not given any further physical interpretation in this work. These parameters were used rather as an adequate mathematical description of the time course of fluorescence decay, one which we attempted to reproduce with kinetic modeling of PSII excited-state dynamics.

*Kinetic Modeling.* Two different physical models were used to describe the PSII fluorescence decay kinetics obtained in this study in an attempt to reveal the molecular mechanisms which give rise to the difference between the PSI-less control and the H117T mutant. In the first approach, we tested the reversible radical pair (RRP) model for excitation energy transfer, primary charge separation, and charge stabilization in PSII (*30*). In this analysis we assumed that exciton equilibration in PSII is fast and completed in less than 20 ps in both the control and the mutant. The RRP model predicts biexponential decay kinetics due to the contribution of reversible electron-transfer steps to the fluorescence decay. Rate constants for the primary photophysical and photochemical processes in PSII (excitation trapping by reaction centers, $k_{PC}^{trap}$; charge recombination, $k_{PC}^{-}$, and charge stabilization by irreversible electron transfer to $Q_A$, $k_{ST}$) derived from the kinetic modeling of the data obtained from isolated thylakoids are summarized in Table 1. In the framework of the RRP model, the difference between the control and H117T was described well by a decrease in the apparent rate constant for charge separation (20%) and an increase in the rate constant for charge recombination (25%). It was not possible to fit the data well if only one of these two rate constants was allowed to vary between the control and the H117T mutant (not shown). This suggests that the H117T mutation induced more complex changes in the photochemistry of PSII than were expected to appear as a result of a simple disruption of energy transfer between the antenna and reaction center. However, there is room for uncertainty within the RRP model as it is not possible to distinguish between the effect of a change in the rate constant for charge separation and a change in the rate of energy transfer from antenna to the reaction center as both

of these processes are described by one rate constant, $k_{PC}^{trap}$. Note that for a change in energy transfer the contribution of thermal equilibration to the overall fluorescence decay might be large, which would make the RRP model inappropriate for modeling the fluorescence decay kinetics of the H117T mutant.

To address this problem, we attempted to describe our experimental fluorescence decay data with a more detailed kinetic model which explicitly included energy transfer between the antenna Chls and the reaction center core pigments. In these simulations we assumed that the molecular rate constant for charge separation ($k_{PC}$) was not affected by the mutation. The rate matrix of pairwise transfer and unimolecular decay rates between all pigments in the CP43−CP47−D1−D2 complex was constructed by consideration of the following physical model. CP43 was assumed to bind 14 chlorophylls, and in accordance with recent structural data these chlorophylls were randomly distributed in two layers within a cylinder of 39 Å diameter and 40 Å height. The two layers of pigments were separated by 8 Å (*18*). The same model was used for CP47. Positions and orientations of the electron-transfer pigments were taken from a model of the D1−D2 reaction center (*5*) (PDB file 1dop). P680 was modeled as a single dipole located at the center of mass of the special pair with double oscillator strength. The two peripheral accessory chlorophylls, $Chl_Z$ and $Chl_D$, were positioned at a distance of 2 Å (length of coordination bond) from histidines 117-D2 and 118-D1. Orientations of these Chls were optimized for the best rate of excitation transfer to the reaction center core pigments. At the most favorable orientation the rate constant of this process was still found to be relatively slow, about 9 $ps^{-1}$. The two cylinders representing CP43 and CP47 were located at either side of the D2−D2 heterodimer to mimic the structural data described in ref *31*. Orientations of pigments in the models of CP43/47 were randomly assigned, and then the models were checked for the absence of uncoupled Chls. After assembling the model for the D2−D2−CP43−CP47 supercomplex, we also ensured that transfer rates from CP43/47 to the peripheral chlorophylls ($Chl_Z$, $Chl_D$) of the reaction center were fast. Absorption maxima and relative amounts of the chlorophyll spectral forms were taken from ref *32* and randomly distributed over the pigments. For our simulation we calculated transfer rates between all pairs of pigments using the analytical expression of Shipman and Housman (*33*) assuming a refractive index of 1.3 and a Stokes shift of 150 $cm^{-1}$. Reversible charge separation and charge stabilization were modeled by introducing two additional, sequentially connected, nonfluorescing sites, corresponding to the primary radical pair and $Q_A$. Rate constants for charge recombination and charge stabilization generated from the RRP model were used as starting parameters to fit the model to the experimental data for control samples. However, in the current model, $k_{PC}$ represents the molecular rate constant for charge separation which is related to $k_{PC}^{trap}$ from the RRP model by the expression $k_{PC} = k_{PC}^{trap}(\mathbf{P}_{P680})^{-1}$, where $\mathbf{P}_{P680}$ is the $^1P680^*$ state normalized to the total amount of excitation in the system. For the control thylakoids a fit of good quality was obtained with $k_{PC} = 0.94$ $ps^{-1}$, $k_{PC}^{-} = 5.9$ $ns^{-1}$, and $k_{ST} = 2.3$ $ns^{-1}$. The value of the rate constant for charge stabilization is in correspondence with results obtained with the RRP model and with results of previous studies, while the other two rates are faster (*30*, *34*−*36*). This result is a consequence of the slow transfer step from the peripheral Chls and will be discussed later. We then attempted to fit the fluorescence decay kinetics of the H117T mutant by setting $k_{PC}$, $k_{PC}^{-}$, and $k_{ST}$ to the same values obtained from our analysis of the control samples and removing the peripheral chlorophyll from D2. This perturbation slowed the model decay kinetics to a much larger extent than we experimentally observed in the H117T mutant. We then tried to fit the mutant decay by changing only the orientation of the peripheral Chl of D2 (rotating it around the axis perpendicular to the membrane plane). As shown in the insert to Figure 4 (solid line), the quality of these fits was extremely poor ($\chi^2 > 7$). When $k_{PC}^{-}$ was also allowed to vary, the correspondence between the calculated decay curves and the experimental fluorescence kinetics was improved substantially (Figure 4, insert, dashed line). From this model we estimated $k_{PC}^{-} = 7.3$ $ns^{-1}$ and $k_{ChlHis117\rightarrow RC} = 42$ $ns^{-1}$ in the H117T mutant.

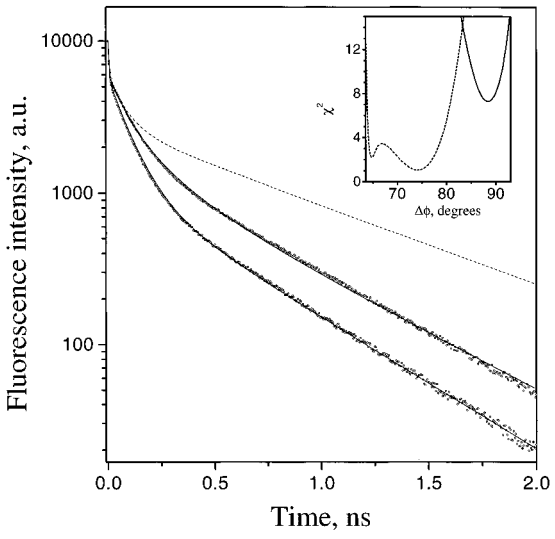


FIGURE 4: PSII decay kinetics, components $\tau_1-\tau_3$ (open circles), obtained from a global lifetime analysis of the PSI-less control (lower trace) and H117T mutant in PSI-less background (upper trace) thylakoids compared to PSII decay calculated with the detailed kinetic model (solid lines). The dashed line represents fluorescence decay predicted by the model if the Chl at His117 was removed. The insert shows $\chi^2$ values for the fits of the mutant kinetics by changing only the angle of the ChlHis117 (solid line) and the angle along with the rate constant for charge recombination (dashed line). See text for details.

*Absorbance Cross Sections.* Effective absorption cross sections, as a measure of the functional antenna size of PSII, provide an independent way of getting information about excitation energy transfer. Typical flash saturation curves constructed from the pump−probe technique are shown with the best fit to each data set using the single-hit Poisson distribution (Figure 5). For each curve, fluorescence arising from the probe flash increases from the minimal yield ($F_0$—all PSII centers open) to the maximal yield ($F_{sat}$—all centers closed by single turnover laser pump flashes). Fluorescence values have been normalized by setting the minimal fluorescence to unity. A single-component Poisson distribution gave excellent fits to our data obtained from H117T mutant cells. When data from the control strain were analyzed, a two-component Poisson distribution function was necessary

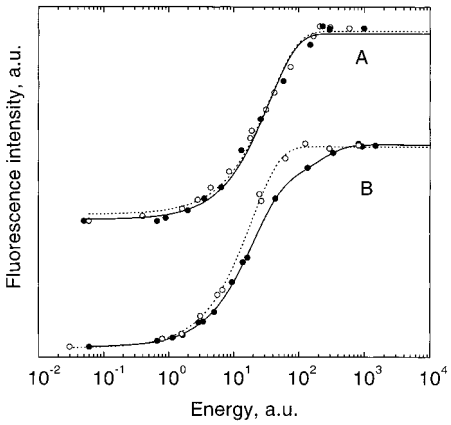


FIGURE 5: Flash saturation curves measured with the pump−probe technique. The excitation wavelength was 440 nm (A) or 665 nm (B). Open circles: H117T mutant in PSI-less background cells. Solid circles: PSI-less control cells. The lines represent the best fit to each data set using a one- or two-component single-hit Poisson distribution; dashed lines are for the H117T mutant in PSI-less background cells, and solid lines are for the PSI-less control cells. The curves in (A) are displaced vertically relative to the curves in (B) by arbitrary amounts.

Table 2: Absorption Cross Sections of the H117T Mutant in PSI-less Background Cells Relative to the PSI-less Control Cells Calculated from Poisson Distribution Fits to Flash Saturation Curves Measured at Different Wavelengths (see Materials and Methods) and Predicted from Fluorescence Decay Data Using the Detailed Kinetic Model for PSII[a]

| | cross section, au | | |
|---|---|---|---|
| | control | | H117T |
| expt (630 nm) | 1.0 (76) | 0.15 (24) | 1.13 (100) |
| expt (665 nm) | 1.0 (76) | 0.1 (24) | 1.01 (100) |
| expt (440 nm) | 1.0 (100) | | 0.97 (100) |
| prediction | 1.0 (100) | | 0.98 (100) |

[a] Two-component Poisson fits were required for the PSI-less control cells for data collected at 630 and 665 nm excitation [relative amplitudes (in %) are shown in parentheses]. The predicted cross sections were calculated from an appropriate numerical solution of eq 3. The standard error for the measured cross sections was 6%.

for satisfactory fits to the data obtained for phycocyanin excitation with a 665 nm pump wavelength. A small fraction of PSII (about 24%) was characterized by a 7-fold smaller functional antenna size than the major population of PSII, indicating the presence of a small population of PSII lacking phycobilisomes. There was no evidence for such a population in the H117T mutant cells. This is consistent with the larger amount of phycobilins relative to chlorophyll in this mutant compared to the control as observed from their absorption spectra (data not shown). Absorption cross sections for all pump−probe experiments are compiled in Table 2. Absorption cross sections are expected to decrease with respect to the control value for samples with quenched fluorescence. A decrease of the effective absorption cross section would be consistent with the decreased half-saturated oxygen evolution yield observed in an earlier study of the H117T mutant (*16*). Interestingly, the absorption cross section of H117T for phycobilin excitation increased by 13% and remained the same as the control for chlorophyll excitation.

## DISCUSSION

Previous work on the H117T mutant of the D2 protein in PSII showed the mutant to be characterized by decreased variable fluorescence at room temperature and by decreased fluorescence emission yield at 695 nm relative to 685 nm at 77 K. That work indicated the H117T mutant had a quenched maximal Chl *a* fluorescence yield ($F_m$) at room temperature and a quenched emission yield at 695 nm at 77 K. The accumulation of chlorophyll cation in H117T in the light was suggested as a molecular mechanism for the quenching. A number of experimental data presented in this study (time-resolved fluorescence measurements performed at room temperature and measurements of absorption cross sections) clearly indicate that the maximal fluorescence yield of the H117T mutant is not quenched. We have found that the decreased variable fluorescence, characteristic of this mutant, arises from an increase in the yield of fluorescence from open reaction centers in the dark ($F_0$).

Analysis of the picosecond decay kinetics revealed that the $F_0$ fluorescence yield of the mutant was elevated because both (i) the contribution of the slow (1.8 ns) decay component was higher and (ii) the decay of PSII with open reaction centers was slower. On the basis of its lifetime, amplitude, and similarity to decay in the PSI/PSII-less control, we have assigned the 1.8 ns component to an additional chlorophyll population which does not transfer excitation to PSII. Alternatively, it is possible that some of this decay component arises from a population of closed PSII centers.

The slower PSII-associated decay kinetics in the H117T mutant strongly suggested that excitation energy transfer between the antenna and the electron-transfer pigments was impaired as a result of substitution of His117 in the D2 protein. However, both kinetic models used in this study failed to explain the difference in PSII-associated fluorescence decay kinetics between control and H117T by impairment of excitation energy transfer only. Results of our kinetic model simulations suggested that the H117T mutation induced more complex changes in the primary photochemistry of PSII and that an increase in the rate constant for charge recombination from 5.9 to 7.3 $ns^{-1}$ was required as well as a decrease in the rate constant for excitation energy transfer from the peripheral chlorophyll (Chl at His117−D2) to the electron-transfer pigments. Recent studies on primary processes in PSII and purple bacteria (*37*, *38*) suggest that the free energy difference for charge separation is time dependent rather than being a static value. The reaction of charge stabilization can be pictured as a continuous process where the protein matrix reacts to the electrostatic forces caused by the sudden creation of a pair of ions. Replacement of the amino acid and a change of orientation and position of its liganded chromophore in the D2 protein could affect protein dynamics by limiting the number of degrees of freedom and thus slowing down the relaxation of the radical pair and increasing the probability of the back-reaction.

To further test our kinetic model for PSII, we used it to calculate the expected change in the effective absorbance cross section between the control and H117T mutant and then compared this to the measured changes in the effective cross section. As the pigment composition of PSII is expected to be the same for both the control and the mutant, the relative changes of the effective absorption cross section correspond to changes in energy transfer and/or electron-transfer efficiency which affect the yield of the photoproduct. Our detailed kinetic model allowed us to calculate the yield

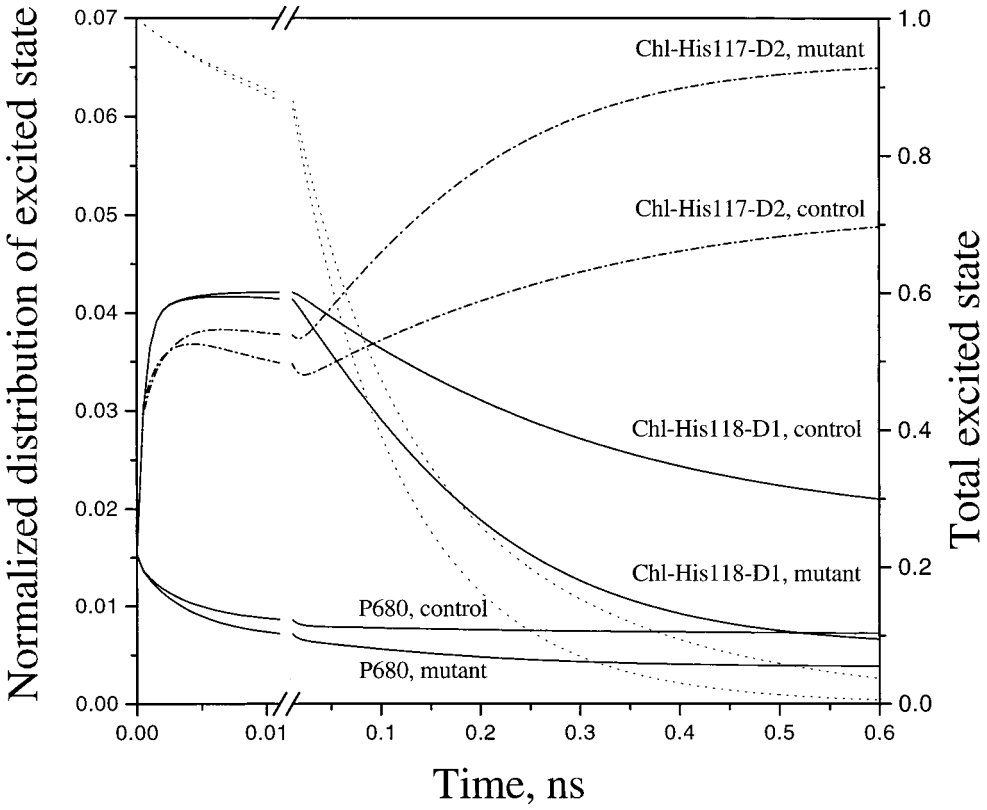


FIGURE 6: Excited-state decay (dotted lines) and time-resolved excited-state distributions (solid and dash-dotted lines) calculated from the detailed kinetic model (eq 3) with 664 nm excitation at room temperature. The excited-state distributions are presented for the P680 reaction center and two peripheral chlorophylls and have been normalized to the total amount of excited state remaining at any given time.

of the photoproduct explicitly. Intuitively, it is clear that if excitation energy transfer between the antenna and the reaction center is substantially slowed, but is still faster than the rate of the photochemical losses, the yield of the photoproduct would not significantly decrease. Model simulations predicted the yield of photochemistry to be 0.95 for the PSI-less control and 0.93 for the H117T mutant, a result in agreement with our observation of no change in the effective absorbance cross section for excitation of chlorophyll *a*.

An interesting finding of our kinetic simulations, based on the available structural information for PSII, is a slow (>8 ps) excitation transfer from antenna chlorophylls to the electron-transfer pigments. This finding raises an important question: is the equilibrium radical pair description appropriate for the H117T mutant or even for wild-type PSII? This question can be addressed with simulations of excitation dynamics in our model systems. The detailed kinetic model allows us to follow the distribution of the total excited state over any of the pigment molecules in CP43, CP47, or the reaction center. One way to follow excited-state dynamics in the antenna is to look at the establishment of transfer equilibrium (TE). By definition, TE is the state of the system at which the fraction of the excited state on any pigment normalized to the total excited state remaining on the model will remain constant. Establishment of TE can be monitored by plotting the fraction of the remaining excited state on any given pigment in the system, as shown in Figure 6. The data in Figure 6 clearly show a rapid depletion of excited state on P680 similar to that observed in PSI and bacterial RC. Our model also predicts that equilibration in PSII (monitored by excited-state distribution on peripheral chlorophylls of the RC) is not complete within the time window of the photochemically limited lifetime. The deviation from equilibrium becomes much more pronounced in the mutant. These results question the application of the RRP model to control PSII and clearly negate its application to the mutant. Our simulations predict a deviation in excitation distribution from the Boltzmann equilibrium distribution; however, owing to a strong spectral overlap between the RC core and the CP43/47 antenna pigments, it would be very difficult to observe it experimentally. Discrepancies between the RRP model and our detailed kinetic model become obvious when these two models are used to extrapolate the molecular rate of charge separation based on the measured fluorescence decay kinetics. The intrinsic charge separation rate 3 $ps^{-1}$, calculated using the RRP model and experimental results of our study, is in good agreement with results of the previous estimations based on application of RRP to the analysis of intact PSII (*30*) or isolated D1−D2 reaction centers (*34*, *39*). To date, values for the intrinsic rate of charge separation in intact PSII have only been derived from applications of the RRP model. In the present study our detailed kinetic model for PSII required a $k_{PC}$ of about 1 $ps^{-1}$ in our simulations to make them fit experimental data. Recently, an extension of the RRP model which considered two pools of antenna pigments with a 15 ps energy-transfer time between them was used to describe excitation transfer in PSII membrane particles (*40*). In some sense this model is similar to our detailed kinetic model which revealed the presence of pigment pools with an approximately 8 ps transfer time between them. Analysis of PSII decay kinetics using the extended RRP model as well as our detailed kinetic model both predict a rate of charge separation faster than 3 $ps^{-1}$.

Therefore, we suggest that the intrinsic primary charge separation in intact PSII may be faster than in isolated D1−D2 reaction centers. However, we leave a detailed scrutiny of our kinetic models for the D1−D2−CP43−CP47 complex for a subsequent report.

## CONCLUSIONS

In this study we have presented a physically reasonable model which explains the difference between fluorescence decay kinetics of the wild-type PSII and PSII with a modified chlorophyll binding site at the His117 residue of D2. The kinetic model used for this purpose is based on the available PSII spectral and structural information. In the framework of this model the difference between PSII decay kinetics of the normal PSII and the mutant at room temperature were described well with only two fitting parameters. The validity of our concept was further supported by the ability of the model to predict the effect of mutation on the effective absorption cross section. This study has important implications for the understanding of excited-state dynamics in PSII. The results of our study rule out quenching of excitation by a chlorophyll cation radical as a mechanism responsible for the lower efficiency of excitation energy utilization in the H117T mutant and demonstrate the importance of the Chl associated with His117 of the D2 protein for excitation energy transfer to the PSII electron-transfer pigments and for the effective stabilization of the primary radical pair.

## ACKNOWLEDGMENT

We thank Wim Vermaas for a generous gift of the H117T mutant and PSI-less control of *Synechocystis* sp. PCC 6803 and for helpful suggestions with the work and manuscript. We are grateful to Tom Owens for fruitful discussions and for "encouraging" us to improve our kinetic modeling of PSII. We also thank the Brock Electronics and Machine shops for their excellent technical assistance.

## REFERENCES

1. Hankamer, B., Barber, J., and Boekema, E. J. (1997) *Annu. Rev. Plant Physiol. Plant Mol. Biol. 48*, 641−671.
2. Nanba, O., and Satoh, K. (1987) *Proc. Natl. Acad. Sci. U.S.A. 84*, 109−112.
3. Bricker, T. M. (1990) *Photosynth. Res. 24*, 1−13.
4. Michel, H., and Deisenhofer, J. (1988) *Biochemistry 27*, 1−7.
5. Svensson, B., Etchebest, C., Tuffery, P., van Kan, P. J. M., Smith, J., and Styring, S. (1996) *Biochemistry 35*, 14486−14502.
6. Ruffle, S. V., Donnelly, D., Blundell, T. L., and Nugent, J. H. A. (1992) *Photosynth. Res. 34*, 287−300.
7. Eijckelhoff, C., and Dekker, J. P. (1995) *Biochim. Biophys. Acta 1231*, 21−28.
8. Eijckelhoff, C., van Roon, H., de Groot, M.-L., van Grondelle, R., and Dekker, J. P. (1996) *Biochemistry 35*, 12864−12872.
9. Schelvis, J. P. M., van Noort, P. I., Aartsma, T. J., and Van Gorkom, H. J. (1994) *Biochim. Biophys. Acta 1184*, 242−250.
10. Zheleva, D., Hankamer, B., and Barber, J. (1996) *Biochemistry 35*, 15074−15079.
11. Vacha, F., Joseph, D. M., Durrant, J. R., Telfer, A., Klug, D., Porter, G., and Barber, J. (1995) *Proc. Natl. Acad. Sci. U.S.A. 92*, 2929−2933.
12. Mulkidjanian, A. Y., Cherepanov, D. A., Haumann, M., and Junge, W. (1996) *Biochemistry 35*, 3093−3107.
13. Koulougliotis, D., Innes, J. B., and Brudvig, G. W. (1994) *Biochemistry 33*, 11814−11822.
14. Stewart, D. H., Cua, A., Chisholm, D. A., Diner, B., Bocian, D. F., and Brudvig, G. W. (1998) *Biochemistry 37*, 10040−10046.
15. Pakrasi, H. B., and Vermaas, W. (1992) in *The photosystems: structure, function and molecular biology* (Barber, J., Ed.) Vol. 11, pp 231−256, Elsevier Science Publishers, Amsterdam.
16. Lince, M. T., and Vermaas, W. (1998) *Eur. J. Biochem. 256*, 595−602.
17. Rhee, K. H., Morris, E. P., Zheleva, D., Hankamer, B., Kuhlbrandt, W., and Barber, J. (1997) *Nature 389*, 522−526.
18. Rhee, K. H., Morris, E. P., Barber, J., and Kuhlbrandt, W. (1998) *Nature 396*, 283−286.
19. Tang, X.-S., and Diner, B. (1994) *Biochemistry 33*, 4594−4603.
20. Samson, G., and Bruce, D. (1996) *Biochim. Biophys. Acta 1276*, 147−153.
21. Mauzerall, D., and Greenbaum, N. L. (1989) *Biochim. Biophys. Acta 974*, 119−140.
22. Vasil'ev, S., Wiebe, S., and Bruce, D. (1998) *Biochim. Biophys. Acta 1363*, 147−156.
23. Vasil'ev, S., and Bruce, D. (1998) *Biochemistry 37*, 11046−11054.
24. Mullineaux, C. W., and Holzwarth, A. R. (1993) *Biochim. Biophys. Acta 1183*, 345−351.
25. Mullineaux, C. W., and Holzwarth, A. R. (1991) *Biochim. Biophys. Acta 1098*, 68−78.
26. Jean, J. M., Chan, C.-K., Fleming, G. R., and Owens, T. G. (1989) *Biophys. J. 56*, 1203−1215.
27. Holcomb, C. T., and Knox, R. S. (1996) *Photosynth. Res. 50*, 117−131.
28. Schatz, G. H., Brock, H., and Holzwarth, A. R. (1987) *Proc. Natl. Acad. Sci. U.S.A. 84*, 8414−8418.
29. Hodges, M., and Moya, I. (1988) *Biochim. Biophys. Acta 935*, 41−52.
30. Schatz, G. H., Brock, H., and Holzwarth, A. R. (1988) *Biophys. J. 54*, 397−405.
31. Hankamer, B., Morris, E. P., and Barber, J. (1999) *Nat. Struct. Biol. 6*, 560−564.
32. Jennings, R. C., Bassi, R., Garlaschi, F. M., Dainese, P., and Zucchelli, G. (1993) *Biochemistry 32*, 3203−3210.
33. Aro, E.-M., Virgin, I., and Andersson, B. (1993) *Biochim. Biophys. Acta 1143*, 113−134.
34. Wasielewski, M. R., Johnson, D. G., Seibert, M., and Govindjee (1989) *Proc. Natl. Acad. Sci. U.S.A. 86*, 524−528.
35. Wiederrecht, G. P., Seibert, M., Govindjee, and Wasielewski, M. R. (1994) *Proc. Natl. Acad. Sci. U.S.A. 91*, 8999−9003.
36. Vasil'ev, S., Bergmann, A., Redlin, H., Eichler, H.-J., and Renger, G. (1996) *Biochim. Biophys. Acta 1276*, 35−44.
37. Konermann, L., Gatzen, G., and Holzwarth, A. R. (1997) *J. Phys. Chem. 101*, 2933−2944.
38. Peloquin, J. M., Williams, J. C., Lin, X., Alden, R. G., Taguchi, A. K. W., Allen, J. P., and Woodbury, N. W. (1994) *Biochemistry 33*, 8089−8100.
39. Donovan, B., Walker, L. A., Kaplan, D., Bouvier, M., Yocum, C. F., and Sension, R. J. (1997) *J. Phys. Chem. 101*, 5232−5238.
40. Dau, H., and Sauer, K. (1996) *Biochim. Biophys. Acta 1273*, 175−190.

BI000476V